Front. Agr. Sci. Eng. 2022, 9(1): 120–132 https://doi.org/10.15302/J-FASE-2021410

RESEARCH ARTICLE

PRODUCTION OF NEW WAP-8294A CYCLODEPSIPEPTIDES BY THE BIOLOGICAL CONTROL AGENT *LYSOBACTER ENZYMOGENES* OH11

Jing ZHU[1,2], Yuan CHEN[1], Liangcheng DU (✉)[1]

1 Department of Chemistry, University of Nebraska-Lincoln, Lincoln, Nebraska 68588, USA.
2 State Key Laboratory of Microbial Technology, Shandong University, Qingdao 266237, China.

KEYWORDS

biocontrol, biosynthesis, *Lysobacter*, natural products, WAP-8294A

HIGHLIGHTS

- *Lysobacter enzymogenes* mutants were generated for WAP-8294A biosynthesis.
- Essential and non-essential accessory genes for WAP-8294A biosynthesis were determined.
- Six new WAP-8294A analogs were identified using UHPLC-HR-MS/MS.
- Three deoxy analogs were detected supporting the function of ORF4 in asparagine hydroxylation.

Received January 6, 2021;
Accepted June 15, 2021.

Correspondence: ldu3@unl.edu

GRAPHICAL ABSTRACT

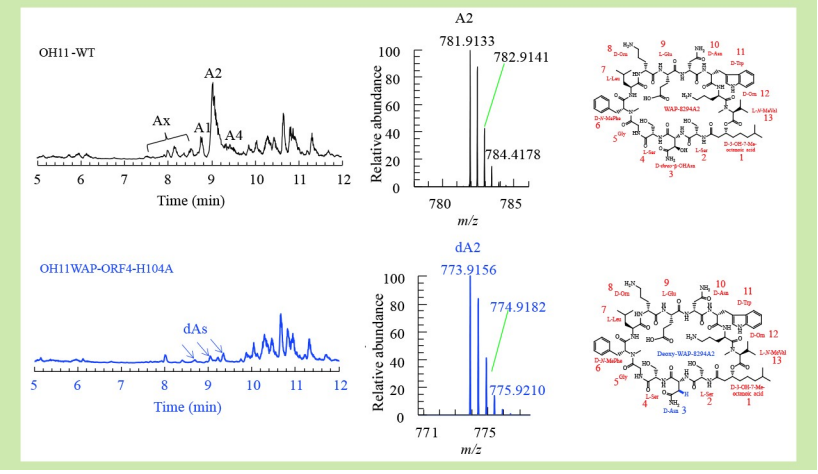

ABSTRACT

Naturally-occurring environmental microorganisms may provide 'green' and effective biocontrol tools for disease management in agricultural crops. Due to the constant threat of resistant pathogens there is a pressing and continual need to search for new biocontrol tools. This study investigated the production of new analogs of WAP-8294A compounds by the biocontrol agent *Lysobacter enzymogenes* OH11 through biosynthetic engineering. WAP-8294As are a family of natural cyclic lipodepsipeptides with potent activity against Gram-positive bacteria. A series of genetic manipulations was therefore conducted on the accessory genes in the WAP biosynthetic gene cluster. The resulting strains containing a single-point mutation in ORF4, which was predicted to encode a 2-ketoglutarate dependent dioxygenase, produced deoxy-WAP-8294As. This result provides evidence for the function of ORF4 in catalyzing β-hydroxylation of the D-asparagine residue in WAP-8294As. In addition, six new analogs of WAP-8294As were identified by UHPLC-HR-MS/MS. This is the first attempt to produce new WAP-8294As in *Lysobacter* and shows that the spectrum of the biocontrol compounds may be expanded through the manipulation of biosynthetic genes.

1 INTRODUCTION

The search for safe and effective pesticides for the protection of crops has become increasingly reliant on natural products as a source for novel chemistry. Environmental microorganisms that produce bioactive natural products are important tools in pest management. Several pesticidal products such as Avermectin and Spinosad derived from microorganisms have been commercialized. The BT endotoxins have become an integral component of strategies to develop transgenic plants that express insecticidal proteins and have been very successful in the control of insect pathogens. These products are often classified by the US Environmental Protection Agency as reduced-risk pesticides that pose little risk to human health and the environment. The identification and production of natural products with new chemistry and unique mode of action are critical steps in combating the constant emergence of resistant pathogens.

Lysobacter are gliding Gram-negative bacteria ubiquitously inhabiting soils and waters[1]. Several species of *Lysobacter* are prolific producers of extracellular lytic enzymes and are emerging as promising sources of new bioactive natural products[2]. Of these, *Lysobacter enzymogenes* is a microbial species of ecological and agricultural relevance[3,4]. *L. enzymogenes* strain C3 exhibited field efficacy against diseases of turfgrass, Bipolaris leaf spot caused by *Bipolaris sorokiniana*[5], brown patch caused by *Rhizoctonia solani*[3], stem rust caused by *Puccinia graminis* and bean rust caused by *Uromyces appendiculatus*[6]. It also reduced the severity of Kentucky bluegrass summer patch caused by *Magnaporthiopsis poae*, suppressed damping-off of sugar beet caused by *Pythium ultimum* and Fusarium head blight caused by *Fusarium graminearum* (*Gibberella zeae*)[7,8].

Several types of bioactive natural products from *Lysobacter* have been identified including polycyclic tetramate macrolactams (PoTeM), cyclic lipodepsipeptides, cephem-type β-lactams, and phenazines[2]. Two strains of *L. enzymogenes*, C3 and OH11, have been extensively investigated due to their production of several structurally distinct and biologically active products such as the PoTeM heat-stable antifungal factor that is responsible for activity against fungi and oomycetes[9–14]. Several nonribosomal peptides isolated from *Lysobacter* such as the cyclic peptides (tripropeptins, WAP-8294As, lysocins, WBP-29479A1 and lysobactin) possess complex chemical structures and exhibit highly potent antibacterial activity[15–23]. Of the cyclic peptides the WAP-8294A family isolated from *Lysobacter* sp. WAP-8294 and *L. enzymogenes* OH11 has potent activity against Gram-positive bacterial pathogens[24–26]. The family consists of a complex of at least 19 closely related cyclic lipodepsipeptides and WAP-8294A2 is the major component. The structure of WAP-8294A2 was determined by mass spectrometry (MS), 1D and 2D NMR, while A1, A4, Ax8, Ax9 and Ax13 were isolated as minor components and identified by ESI-MS/MS[24–26]. The remainder of the family were detected by high-pressure liquid chromatography (HPLC) but their structures are not known due to the extremely low yields.

The biosynthetic gene cluster (BGC) for WAP-8294As from *L. enzymogenes* OH11 has been identified[19]. The BGC contains three structural genes, ORFs 1–3 that encode the multimodular nonribosomal peptide synthetases (NRPS) WAPS1 and WAPS2 and the NRPS-associated protein MbtH (Fig. 1). Clustered with the three structural genes are seven accessory genes, ORFs 4–10, which were predicted to function in the modification, regulation and resistance of WAP-8294As[19]. Various approaches including synthetic biology methods have been used in the genetic manipulation of WAP-8294A BGC[27,28]. However, efforts have focused on increasing the yields of the known compounds. So far, the biosynthetic production of new WAP-8294A analogs in *L. enzymogenes* has not been attempted. Here, we conducted a series of genetic manipulations on the accessory genes and found deoxy analogs of WAP-8294As in single-point mutants. Also, using ultra-HPLC and high-resolution tandem mass spectrometry (UHPLC-HR-MS/MS), we detected six new WAP-8294A compounds in wild type OH11. The results show that the spectrum of biocontrol compounds of *L. enzymogenes* OH11 may be expanded through manipulation of the biosynthetic genes.

2 MATERIAL AND METHODS

2.1 Bacterial strains, plasmids, primers and general DNA manipulations

Two *Escherichia coli* strains were used, XL1-Blue as the host for general plasmid DNA propagation and S17-1 as the conjugal strain to transfer DNA into the wild type *L. enzymogenes* OH11. Plasmid pJQ200SK was the vector for in-frame deletion of OH11 genes and plasmid pEX18 as the vector for mutagenesis of single amino acid residues in biosynthetic genes. Kits from Qiagen (Valencia, CA) were used for general plasmid preparation and DNA gel extraction and all other DNA manipulations were conducted using standard methods. Luria-Bertani (LB) broth medium was used for OH11 growth. Primers used are shown in Table S1.

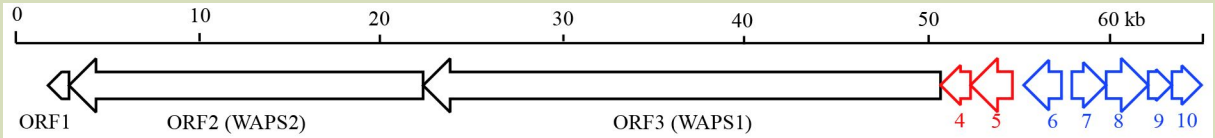

ORF	Predicted function	ORF	Predicted function
ORF1	MbtH	ORF6	Pectin lyase fold/virulence factor
ORF2	NRPS-1 (5 modules)	ORF7	Lytic endopeptidase preproenzyme
ORF3	NRPS-2 (7 modules)	ORF8	TonB-dependent receptor
ORF4	TauD-like dioxygenase	ORF9	SapC-related protein
ORF5	Efflux transporter	ORF10	Pass1-related protein

Fig. 1 The biosynthetic gene cluster for WAP-8294A in *Lysobacter enzymogenes*. ORFs 1–3 are structural genes responsible for the biosynthesis of the peptide scaffold of WAP-8294A compounds, whereas ORFs 4–10 are accessory genes predicted for tailoring, transporting and regulating WAP-8294A compounds.

2.2 Generation of gene deletion mutants and single-point mutants

To construct in-frame deletion vectors two homologous arms of 1.5 kb in length were amplified by PCR from the upstream and downstream regions of the target gene in the OH11 genome using the primers shown in Table S1. The PCR fragments were then cloned into the conjugal vector pJQ200SK by the corresponding restriction enzymes. The constructs were confirmed by DNA sequencing. To construct the vectors for single-point mutagenesis the WAP-ORF4 gene was amplified by PCR from the OH11 genome using the primer pair ORF4-epF(BamH)/ORF4-epR(Hind) and then cloned into vector pET28a, producing plasmid orf4-pET28a. Another run of PCR was conducted using plasmid orf4-pET28a as template and orf4 H104A-F/orf4 H104A-R or orf4 H298A-F/orf4 H298A-R as primers. The PCR fragments were digested with *Dpn*I at 37 °C overnight to specifically digest the methylated and hemimethylated DNA (the parental DNA template). The *Dpn*I-digested products were transformed into XL1-Blue competent cells. The plasmids were extracted from the cells and single-point mutation at H104A or H298A was confirmed by introducing restriction enzyme site *Pae*I or *Eco*52I. The fragment between *Bam*HI and *Hin*dIII from the single-point mutated plasmid pET28a-H104A or pET28a-H298A was released and cloned into vector pEX18.

The constructs for in-frame deletion and single-point mutagenesis were transformed into *E. coli* S17-1 which was grown in LB medium until OD_{600} reached 0.6. *L. enzymogenes* OH11 was cultured in LB containing 10 mmol·L^{-1} $MgCl_2$ until OD_{600} reached 0.6. After centrifugation the pellet from 1 ml OH11 and the pellet from 1 ml S17-1 were separately washed with 10 mmol·L^{-1} $MgSO_4$ and then mixed for intergeneric conjugation. The cells were spread on LB plates containing kanamycin (Km, 100 μg·mL^{-1}) and gentamicin (Gm, 150 μg·mL^{-1}). After growth at 30 °C for 72 h the colonies were transferred to LB plates containing 10% (w/v) sucrose and Km (100 μg·mL^{-1}) at 30 °C for 72 h. The transformants were transferred to LB plates supplemented with Km (100 μg·mL^{-1}) or Km (100 μg·mL^{-1}) + Gm (150 μg·mL^{-1}). The Km-resistant and Gm-sensitive strains were selected as putative in-frame deletion mutants and single-point mutants that were confirmed by diagnostic PCR.

2.3 Extraction of the WAP-8294A compounds from *Lysobacter enzymogenes* strains

Three liquid media (L1M with 2.5% glucose, 2% soybean flour, 0.4% soybean oil, 0.25% NaCl, and 0.5% $CaCO_3$ at pH 7.2; L2M with 0.5% bacteriological peptone, 0.3% yeast extract and 2% glycerol; and L3M with 2% glucose, 0.5% beef extract, 1.6% soybean oil, 0.1% NaCl and 0.1% $CaCO_3$ at pH 8.5) and three solid media (S1M as L1M with 1.5% agar; S2M as L2M with 1.5% agar; and S3M as L3M with 1.5% agar) were used for screening WAP8294A production. After growth in 3 mL LB containing 100 μg·mL^{-1} kanamycin for one day, a 500-μL aliquot of OH11 seed culture was transferred to a 250-mL flask containing 50 mL of liquid medium, L1M, L2M or L3M. The culture was incubated at 28 °C for 2 days with shaking at 200 r·min^{-1}. To extract the metabolites the 50 mL culture broth was collected and adjusted to pH 2.5 with 1 mol·L^{-1} HCl. The supernatant was extracted with 50 mL n-butanol-ethyl acetate (1:1 v/v), containing 0.05% trifluoroacetic acid (TFA). The organic phase was dried with a rotary evaporator (R-200;

Buchi, Flawil, Switzerland) to obtain the crude extract. The extract was dissolved in 1.5 mL methanol containing 0.05% TFA. A 25-μL aliquot of each extract was analyzed by HPLC. Solid cultures were prepared by spreading an aliquot of 150 μL OH11 seed culture on a solid plate and incubating at 28 °C for 2 days. To extract the metabolites the solid culture from three plates was collected and extracted with 50 mL methanol. The methanol extract was dried and redissolved in 1.5 mL methanol containing 0.1% TFA. A 25-μL aliquot of each extract was analyzed by HPLC, or 5 μL by high-resolution UHPLC-ESI-MS/MS. After comparison of the metabolite profile from the liquid cultures and the solid cultures, S2M medium was chosen as the medium for all mutant strains because this medium consistently produced WAP-8294A compounds.

2.4 HPLC and UHPLC-MS/MS analysis of the WAP-8294A extracts

A 25-μL aliquot of each extract was analyzed by HPLC (1220 Infinity LC, Agilent Technologies, Santa Clara, CA) using a reverse-phase column (Cosmosil 5C18-AR-II, 4.6 ID × 250 mm). Water-0.1% TFA (solvent A) and acetonitrile-0.1% TFA (solvent B) were used as the mobile phases with a flow rate of 1.0 mL·min^{-1}. The HPLC program was as follows: 5% to 25% solvent B in solvent A for the first 0 to 10 min, with an increase to 80% B at 25 min, to 100% at 26 min, and back to 5% B at 30 min. The metabolites were detected at 220 nm on a UV detector. The extracts were analyzed by UHPLC-HR-MS by the Proteomics and Metabolomics Facility at the Nebraska Center for Biotechnology at the University of Nebraska-Lincoln, USA. An aliquot of each extract was injected into the column (ACCQ-TAG ULTRA C18 1.7 μm; 2.1 mm × 100 mm, Waters, Milford, MA) on a Vanquish (Thermo Fisher Scientific, Waltham, MA) HPLC at 40 °C at a flow rate of 300 μL·min^{-1}. The solvents were A (0.1% formic acid in 100% LC-MS grade water) and B (0.1% formic acid in 100% acetonitrile) with a gradient as follows: 10% B for 2 min, 10% to 90% B in 12 min, hold at 90% B for 2 min, then back to 10% in 0.5 min. The data were acquired on a QE-HF (Thermo Fisher Scientific) mass spectrometer using a mass range of 375 to 1200 m/z on single charge ions at 60,000 resolution using an AGC target of 3e6 and a maximum ion time of 50 ms. The isolated ions were further fragmented by HCD in data dependent mode (loop count 10, intensity threshold 1e5, dynamic exclusion 10 s) using an isolation window of 1.6 m/z and scanned using a mass range of 120–2000 m/z at a resolution of 15,000.

2.5 Feature-based molecular networking of WAP-8294A extracts

Feature-based molecular networking was conducted using the GNPS platform[29,30]. The MS/MS raw data were converted to the mzML format using ProteoWizard[31] before importing into MZmine2.5.3 software[32] for LC-MS feature detection and alignment. The noise levels of MS1 and MS2 were set to 2E5 and 1E2 according to the low abundance of deoxy-WAPs and the unknown WAPs compounds. The mascot generic format file was uploaded to GNPS and then used to generate a feature-based molecular network. The precursor ion mass tolerance and product ion tolerance were set to 0.01 Da and 0.02 Da. A minimum of eight peaks and a cosine score of 0.6 were allowed. Data were opened and visualized using Cytoscape 3.8.0 software[33]. A ClassDefault layout was used for data visualizations. The nodes, the sizes of which indicate the parent ion abundance, are presented as pie charts with different colors representing the presence of each metabolite in the wild type (OH11) and the ORF4 mutants.

3 RESULTS

3.1 In-frame deletion of the accessory genes in the WAP gene cluster in *Lysobacter enzymogenes* OH11 and analysis of WAP-8294A production in the mutants

To test the idea that new WAP-8294A compounds may be generated through manipulation of the accessory genes clustered with the structural genes (ORFs 1–3 for MbtH and NRPS) we conducted in-frame deletion of the genes in the WAP gene cluster (Fig. 1). First, we deleted each of the four downstream genes, ORFs 6, 7, 9 and 10. ORF8 was omitted because it codes for a TonB-dependent receptor that is unlikely to be related to structural modifications of the compounds[19]. The in-frame deletion mutants, OH11ΔWAP-ORFs 6, 7, 9 and 10, were confirmed by diagnostic PCR using primers designed to distinguish the wild type and the mutants (Fig. S1). The wild type and the mutants were cultured in various media to test that the yield of metabolites with S2M was most suitable for WAP-8294A production under the test conditions. The cultures grew on S2M plates for 2 days and the metabolites were extracted from the whole plates. HPLC shows that the wild type produced WAP8294A1, A2, and A4, with A2 being the predominant WAP8294A compound (Fig. 2(a)). HR-ESIMS confirms the identity of WAP8294A1, A2, and A4, with $[M + 2H]^{2+}$ of m/z 774.9056, 781.9133, and 788.9208, respectively (Table 1, Fig. 2(b,c)). Each of the gene deletion mutants, OH11ΔWAP-ORF6, 7, 9, and 10, produced a similar WAP8294A profile to the wild type. The results indicate that none of the four accessory genes is essential for the WAP-8294A production in OH11. To further confirm this we

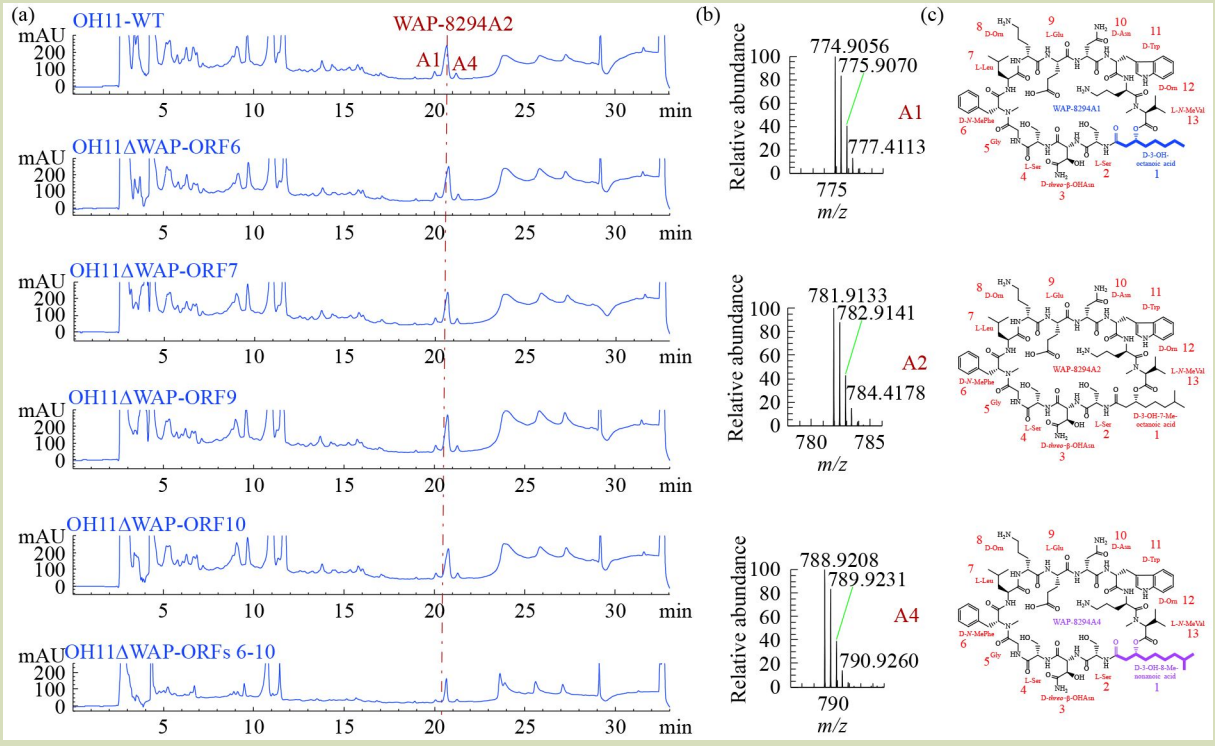

Fig. 2 (a) HPLC analysis of metabolites from *Lysobacter enzymogenes* mutants generated by in-frame deletion of the accessory genes in the WAP gene cluster. (b) Mass spectrometry of the three main WAP-8294A compounds, shown as $[M + 2H]^{2+}$ ions. (c) Chemical structure of WAP-8294A1, A2 and A4. OH11-WT, the wild type; OH11ΔWAP-ORF6, deletion of ORF6; OH11ΔWAP-ORF7, deletion of ORF7; OH11ΔWAP-ORF9, deletion of ORF9; OH11ΔWAP-ORF10, deletion of ORF10; and OH11ΔWAP-ORFs 6–10, quint gene deletion of ORF6 through ORF10.

Table 1 WAP-8294A compounds detected by the ESI MS analyses

Compound	Molecular formula	Change vs A2 building block	Exact mass	Calculated $[M + 2H]^{2+}$	Observed $[M + 2H]^{2+}$
WAP-8294A1	C72H109N17O21	**1**	1547.7984	774.9065	774.9056
WAP-8294A2	C73H111N17O21	–	1561.8140	781.9143	781.9133
WAP-8294A4	C74H113N17O21	**1**	1575.8297	788.9221	788.9208
WAP-8294AZ1	C72H109N17O20	**4**	1531.8035	766.9090	766.9078
WAP-8294AZ2	C72H109N17O20	**2**	1531.8035	766.9090	766.9079
WAP-8294AZ3	C72H108N16O21	**3,4**	1532.7875	767.4010	767.3994
WAP-8294AZ4	C71H107N17O21	**1**	1533.7827	767.8986	767.8971
WAP-8294Ax8	C72H109N17O21	**13**	1547.7984	774.9065	774.9055
WAP-8294AZ6	C73H111N17O23	**11**	1593.8039	797.9092	797.9075
WAP-8294AZ7	C51H73N13O13	**1,2,3,13**	1075.5451	538.7798	538.7794
Deoxy-WAP-8294A1	C72H109N17O20	**1,3**	1531.8029	766.9090	766.9077
Deoxy-WAP-8294A2	C73H111N17O20	**1,3**	1547.8336	773.9168	773.9156
Deoxy-WAP-8294A4	C74H113N17O20	**1,3**	1561.8493	780.9247	780.9231

Note: For A2 building block, see the chemical structure of WAP-8294A2 in Fig. 2(c).

generated a quintet mutant by in-frame deletion of all five downstream genes, ORF6 through ORF10 (including ORF8). The identity of the resulting mutant, OH11ΔWAP-ORFs 6–10, was confirmed by diagnostic PCR (Fig. S1). Notably, HPLC

shows that this quintet mutant still produced the WAP-8294A compounds (Fig. 2(a)). The data verify that these five downstream genes are not essential for WAP-8294A biosynthesis.

Next, we examined the remaining two accessory genes in the WAP gene cluster, ORF4 and ORF5, which appear to form an operon with the structural genes (ORFs 1–3) because the five open reading frames (ORFs 1–5) are tightly coupled in the same transcriptional direction (Fig. 1)[19]. To avoid potential polar effects we generated the mutants by in-frame deleting ORF4 or ORF5 individually. The identities of the mutants, OH11ΔWAP-ORF4 and OH11ΔWAP-ORF5, were confirmed by diagnostic PCR (Fig. S1). HPLC shows that the WAP-8294A compounds were not produced in OH11ΔWAP-ORF4 or OH11ΔWAP-ORF5 (Fig. 3). The results show that both ORF4 and ORF5 are essential for the biosynthesis of WAP-8294A.

3.2 Deoxy-WAP-8294A analogs produced in mutants derived from single-point mutagenesis of ORF4 in the WAP gene cluster

Given that ORF4 was predicted to encode a 2-ketoglutarate dependent dioxygenase that catalyzes either the β-hydroxylation of the D-Asn residue or the β-hydroxylation of the fatty acid moiety in WAP-8294A compounds[19], we postulated that the genetic manipulation of this gene may lead to new WAP-8294A analogs. However, even an in-frame deletion of ORF4 did not result in HPLC detectable WAP-8294A analogs. To further test the function of ORF4 we generated two single-point mutants at the active site residues, His104A or His298A, which maintain ORF4 intact in the mutants with only a single amino acid change. ORF4 is most similar to *E. coli* taurine dioxygenase TauD and related enzymes which contain a conserved **H**X(D/E)-X_{23-26}(T/S)$X_{114-183}$**H**X_{10-13}R motif (the two highly conserved histidine residues are underlined)[34]. His104 and His298 of ORF4 correspond to the two highly conserved histidine residues in this motif. The single-point mutants, OH11WAP-ORF4-H104A and OH11WAP-ORF4-H298A, were confirmed by diagnostic PCR and digestion of a special restriction enzyme site which was introduced at the point mutation site (Fig. S2).

Using HPLC with a UV detector no apparent WAP-8294A compound was detected from either OH11WAP-ORF4-H104A or OH11WAP-ORF4-H298A (Fig. 3). To further examine the metabolites from the single-point mutants we conducted high-resolution LC-MS analysis with a comparison to the metabolites from the wild type. The total ion chromatogram (TIC) of the wild type gave the expected WAP-8294A1, A2 and A4. In addition, the TIC of the wild type showed complexes of peaks (such as Ax) mixed with or flanking the three known compounds (Fig. 4(a)). In contrast, the TIC of the single-point mutant OH11-WAP-ORF4-H104A did not appear to give the main peaks or the peak complexes (such as the Ax complex in Fig. 4(a)). Instead, OH11-WAP-ORF4-H104A produced several minor peaks at the WAP-8294A region on the LC-MS. We examined the three peaks (8.7, 9.1 and 9.4 min) in the mutant because these retention times fall into the region of WAP-8294A compounds. HR-MS shows that the peak at 8.7 min gave *m*/*z* 766.9077 which is coincident with the $[M + 2H]^{2+}$ of deoxy-WAP-8294A1 (calculated 766.9090); the peak at 9.1 min gave *m*/*z* 773.9156 which is consistent with the $[M + 2H]^{2+}$ of deoxy-WAP-8294A2 (calculated 773.9168); the peak at 9.4 min gave *m*/*z* 780.9231 which is in agreement with the $[M + 2H]^{2+}$ of deoxy-WAP-8294A4 (calculated 780.9247) (Fig. 4(b)). Moreover, the extracted ion chromatogram (EIC) of deoxy-WAP-8294A1 mass gave a peak at 8.7 min in mutant OH11-WAP-ORF4-H104A (Fig. 4(c)). Notably, the wild type EIC also contained two peaks with a similar extracted mass to deoxy-WAP-8294A1. As shown below these are new analogs of WAP-8294As (AZ1 and AZ2, see Table 1, Table S2) which have a similar mass (*m*/*z* 766.9090) to deoxy-WAP-8294A1. The EIC of deoxy-WAP-8294A2 mass showed a clear peak at 9.1 min in mutant OH11-WAP-ORF4-H104A but the wild type gave only noise signals in this region (Fig. 4(d)). Similarly, the EIC of deoxy-WAP-8294A4 mass showed a clear peak at 9.4 min in mutant OH11-WAP-ORF4-H104A but the wild type gave only noise signals in this region (Fig. 4(e)). Notably, a small peak at 9.0 min was also shown in the EIC of deoxy-WAP-8294A4 mass which might be an unidentified deoxy-WAP isomer with *m*/*z* in the range 780.9217–780.9237. Taken together, the data demonstrate that the ORF4 single-point mutant was able to produce new WAP-8294A analogs which lack a hydroxyl group of the parent WAP-8294A compounds.

3.3 Deoxy-WAP-8294A analogs missing the β-hydroxyl group on the D-asparagine residue of the parent WAP-8294A compounds

As mentioned above, the 2-ketoglutarate dependent dioxygenase encoded by ORF4 may be responsible for the β-hydroxylation of the D-Asn residue (Fig. 4(f–h)) or the β-hydroxylation of the fatty acid chain in WAP-8294A compounds[19]. The deoxy-WAP-8294A compounds produced in OH11-WAP-ORF4-H104A are most likely due to the lack of the β-hydroxyl group on the D-Asn residue rather than a lack of the β-hydroxyl group on the fatty acid moiety. This is because the β-hydroxyl group on the fatty acid is involved in cyclization of the cyclic lipodepsipeptides, and the lack of this

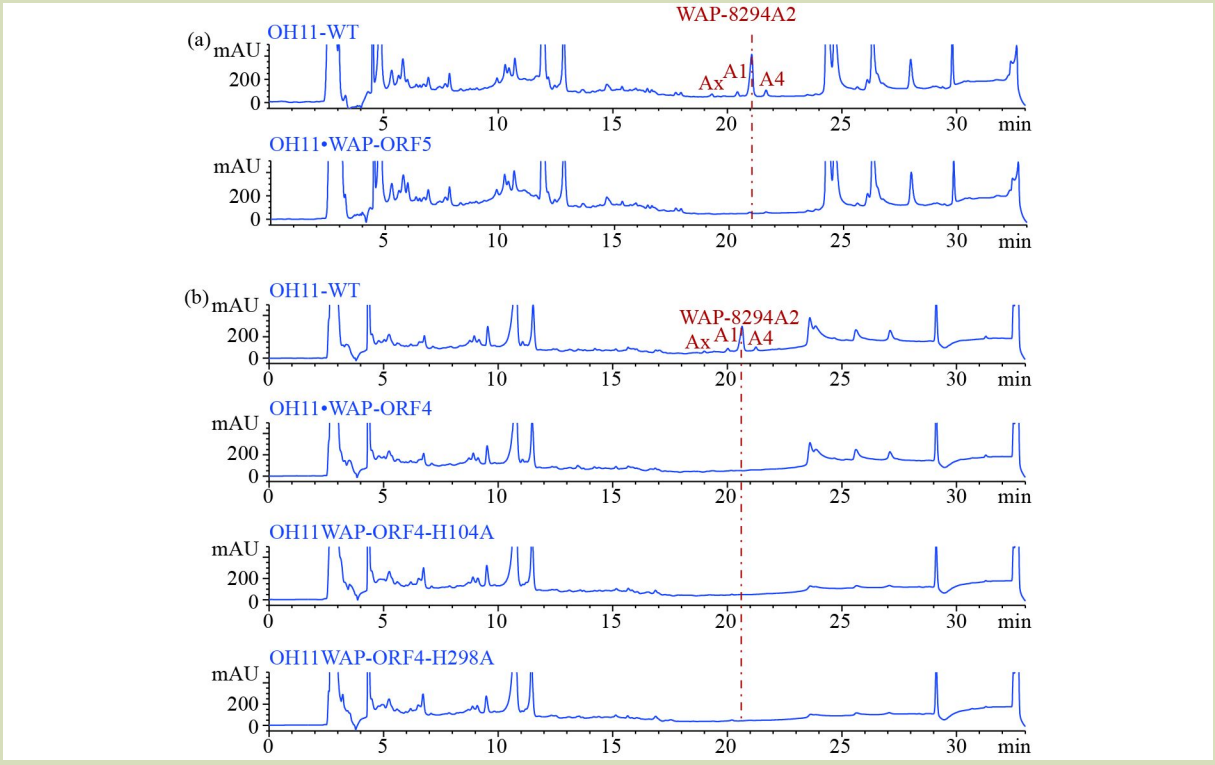

Fig. 3 HPLC analysis of metabolites from *L. enzymogenes* mutants generated by in-frame deletion of ORF5 (a) and by in-frame deletion or single-point mutagenesis of ORF4 in the biosynthetic genes for WAP-8294A (b). OH11-WT, the wild type; OH11ΔWAP-ORF5, deletion of ORF5; OH11ΔWAP-ORF4, deletion of ORF4; OH11WAP-ORF4-H104A, histidine residue at position-104 of ORF4 changed to alanine residue; and OH11WAP-ORF4-H298A, histidine residue at position-298 of ORF4 changed to alanine residue.

β-hydroxyl group would lead to a drastic structural change in the WAP-8294A analogs which would be unlikely to show similar retention times on LC-MS to the known WAP-8294As. To obtain experimental data we analyzed the deoxy-WAP-8294A compounds using UHPLC-HR-MS/MS in comparison with the fragmentation pattern of the parent WAP-8294A compounds (Figs. S3–S4).

The HR-MS/MS fragments of the parent compounds, WAP-8294A1, A2 and A4, from the wild type are summarized in Table S2 which cover the 12 amino acid residues and D-3-OH-fatty acid moiety. The HR-MS/MS profile of deoxy-WAP-8294A1 shared a large number of fragment ions with WAP-8294A1 except at the position of D-*threo*-β-OH-Asn. The deoxy compound showed a reduced mass of 16 at the Asn position, supporting the position of the deoxy at D-*threo*-β-OH-Asn rather than at the D-3-OH-fatty acid moiety (Fig. S4). Similarly, the comparison of the MS/MS fragments from deoxy-WAP-8294A2 with that from WAP-8294A2, and deoxy-WAP-8294A4 with that from WAP-8294A4, further confirm that the β-hydroxyl of the D-Asn residue was missing while the β-hydroxyl of the fatty acid was retained. In addition, we conducted molecular networking analysis of the HR-MS/MS fragments of the WAP metabolites. The results show the presence of deoxy-A1 (*m*/*z* 766.9064), deoxy-A2 (*m*/*z* 773.9146), and deoxy-A4 (*m*/*z* 780.9223) (Fig. 5). In addition, an unknown deoxy-Ax (*m*/*z* 794.9248) was also detected by the molecular networking analysis. In the networking the ions of deoxy-A1, deoxy-A2 and deoxy-A4 clearly shared MS/MS fragments with the respective parent ions from the wild type, A1 (*m*/*z* 774.9044), A2 (*m*/*z* 781.9119), and A4 (*m*/*z* 788.9197). The new deoxy-Ax (*m*/*z* 794.9248) was also connected to a small group of ions that appeared to be new analogs produced in the wild type. Taken together the data obtained from HR-MS/MS confirm the identity of the deoxy-WAP-8294A compounds as shown in Fig. 4(f–h). In addition, the results provide evidence for the function of ORF4 in β-hydroxylation of the D-Asn residue in WAP-8294A biosynthesis.

3.4 New WAP-8294A compounds identified by UHPLC-HR-MS/MS analyses

Encouraged by the identification of the deoxy-WAP8294A

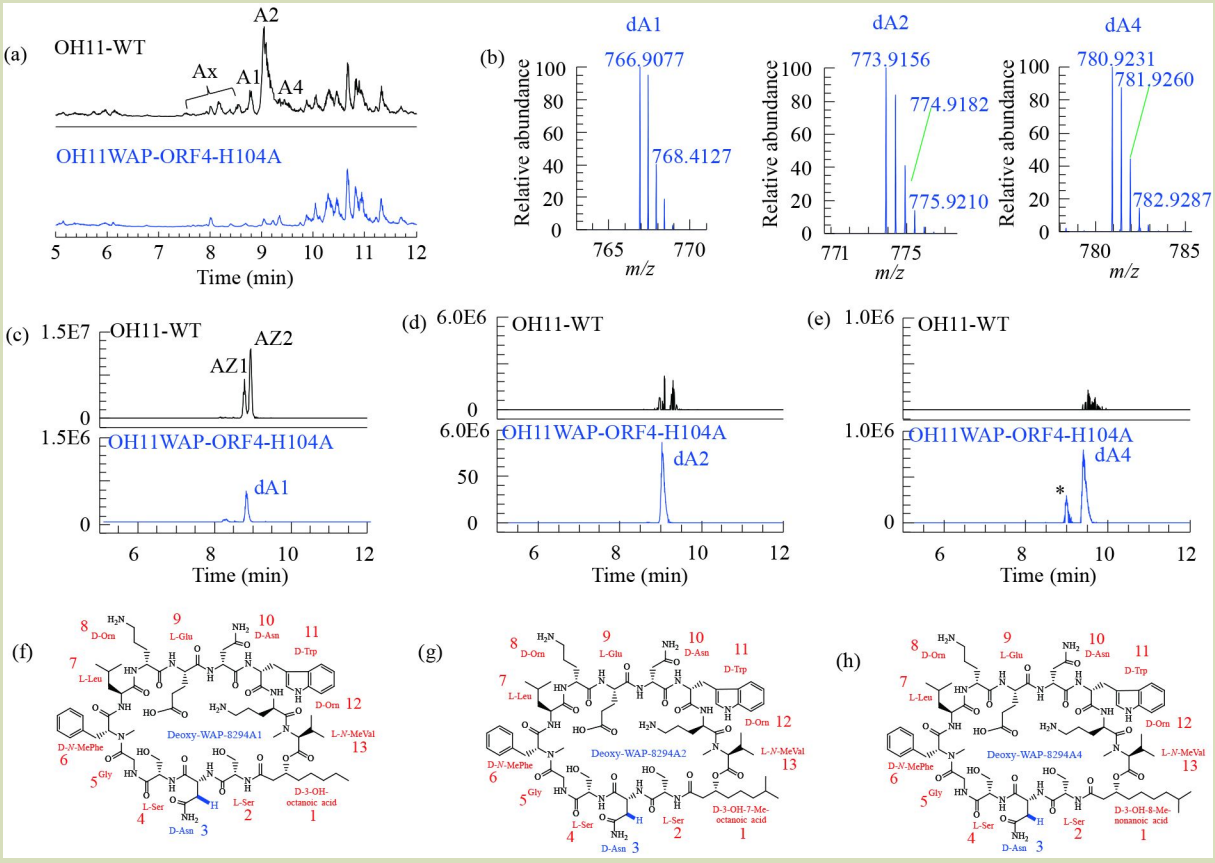

Fig. 4 High-resolution LC-MS of metabolites from the point mutant OH11WAP-ORF4-H104A, with a comparison to the metabolites from the wild type OH11. (a) Total ion chromatogram (TIC) of the wild type OH11-WT and mutant OH11-WAP-ORF4-H104A. The minor metabolite complex is indicated as Ax. (b) MS of deoxy-WAP-8294A1 (expected *m/z* 766.9012, observed 766.9077), deoxy-WAP-8294A2 (expected *m/z* 773.9168, observed 773.9156), and deoxy-WAP-8294A4 (expected *m/z* 780.9247, observed 780.9231) from mutant OH11-WAP-ORF4-H104A. (c) Extracted ion chromatogram (EIC) of deoxy-WAP-8294A1 at 8.7 min. Note that the wild type contains two analogs (AZ1 and AZ2) with the similar mass (*m/z* 766.9090, see Table 1 and Fig. 6) as deoxy-WAP-8294A1. (d) EIC of deoxy-WAP-8294A2 at 9.1 min. (e) EIC of deoxy-WAP-8294A4 at 9.4 min. The asterisk denoted an unidentified deoxy-WAP at 9.0 min, with *m/z* in the range of 780.9231. (f–h) Chemical structure of deoxy-WAP-8294A1, deoxy-WAP-8294A2, and deoxy-WAP-8294A4.

analogs in the ORF4 mutant we set out to examine the minor peaks in the wild type by UHPLC-HR-MS/MS. As shown in Fig. 4(a) the TIC revealed multiple peak complexes present in the metabolites from the wild type. These minor peaks were mixed with or flanking the main peaks (A1, A2, and A4). We detected at least six new minor compounds, WAP-8294AZ1-AZ6, with *m/z* in the range 766.9078 to 797.9075 for $[M + 2H]^{2+}$ (Table 1 and Table S2). UHPLC-HR-MS/MS analyses of each of the six compounds indicate that these belong to the WAP-8294A family, with variations in the amino acid residues (AZ1, AZ2, AZ3 and AZ6) or in D-3-OH fatty acid (AZ4) (Fig. 6(a), Table S2). New compounds were also identified in the molecular networking analysis (Fig. 5). Interestingly, AZ5 appears to be the same as the previously reported minor compound WAP-8294Ax8[25].

In addition to the six compounds we detected an unusual compound, WAP-8294AZ7, which gave *m/z* 538.7794 for $[M + 2H]^{2+}$. This mass is significantly smaller than those of the other family members (Table 1). UHPLC-HR-MS/MS analysis of this compound reveals that AZ7 contains only nine amino acid residues, with the same sequence and composition as the fourth residue (L-Ser) through to the twelfth residue (D-Orn) of WAP-8294A2 (Fig. 6(b)). In the structure of AZ7 the D-3-OH-fatty acid moiety, the first two amino acid residues, L-Ser and D-*threo*-β-OH-Asn, and the last amino acid residue, L-*N*-MeVal, are totally missing. Overall, this study has detected six previously unknown WAP-8294A analogs through UHPLC-HR-MS/MS analysis of the metabolites from the wild type *L. enzymogenes* OH11.

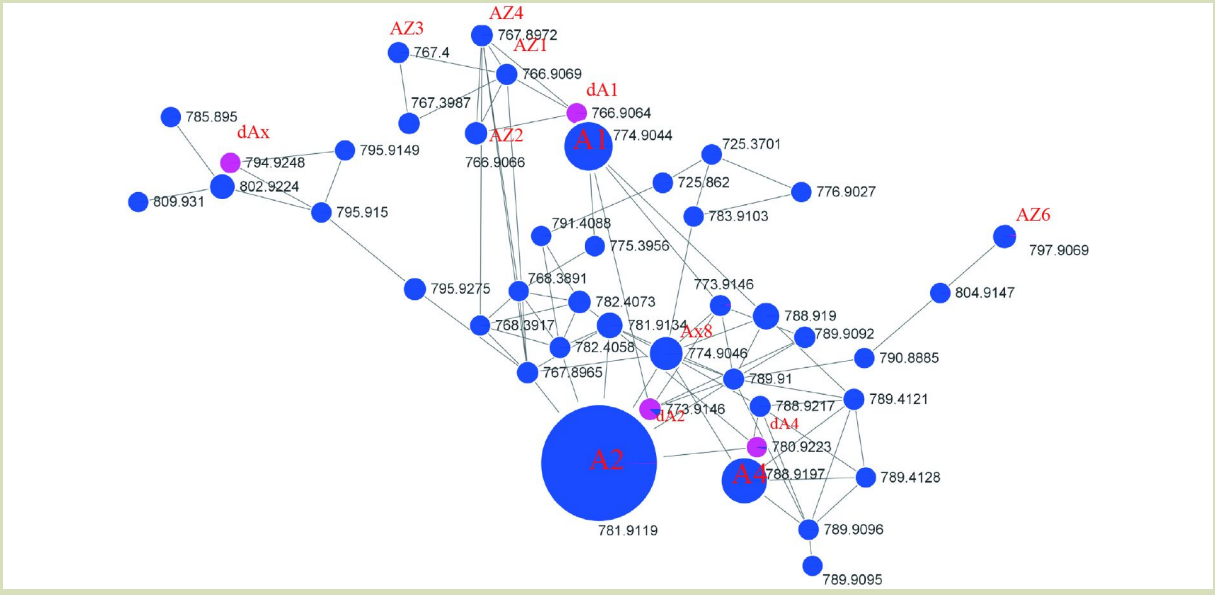

Fig. 5 Feature-based molecular networking of the WAP metabolites isolated from mutant OH11ΔWAP-ORF4 and wild type OH11. The metabolites were analyzed by ultra-high-performance liquid chromatography and high-resolution tandem mass spectrometry (UHPLC-HR-MS/MS) (see Fig. S3 and Fig. S4). The node size indicates semiquantitative differences in metabolite concentrations. Nodes are presented as pie charts with different colors, representing the presence of each metabolite in the wild type (blue) and ORF4 mutant (magenta). Metabolites WAP-8294A1, WAP-8294A2 and WAP8-294A4 are indicated as A1, A2 and A4, respectively. Metabolites deoxy-WAP-8294A1, deoxy-WAP-8294A2 and deoxy-WAP-8294A4 as dA1, dA2 and dA4, respectively. AZ1-AZ6 are the WAP-8294A analogs identified in this study (AZ5 is the same as Ax8, see Fig. 6 and Table 1). Note that a new deoxy-WAP-8294Ax (*m/z* 794.9248, in magenta) was also identified in the networking analysis.

4 DISCUSSION

We previously identified the biosynthetic gene cluster for WAP-8294As from *L. enzymogenes* OH11 and proposed a biosynthetic pathway for WAP-8294As, which are assembled on the giant NRPS enzyme complex encoded by ORFs 1–3[19]. We investigated the mechanisms by which the D-3-OH-fatty acids are incorporated into the amino acid scaffold[35]. We also attempted to increase the yield of WAP-8294As using promoter replacement, CRISPR/dCas9 and gene refactoring[28]. However, new WAP-8294A analogs have not been produced using biosynthetic approaches. Here, we first conducted a series of in-frame deletion of the accessory genes downstream of the three structure genes, ORFs 1–3. This strategy would minimize potential polar effects on the flanking genes. Several gene disruption mutants had previously been generated through inserting a plasmid construct containing the homologous region of ORFs 5, 6 or 8[19]. Our results from in-frame gene deletion of a single gene, ORFs 6, 7, 9 and 10, or all five genes, ORFs 6–10, show that these accessory genes are not essential for biosynthesis. In contrast, in-frame deletion of ORF5 or ORF4 resulted in no WAP-8294A production (Fig. 3), suggesting that the efflux pump encoded by ORF5 and the dioxygenase encoded by ORF4 are essential. These findings are consistent with our recent study in which an overexpression of the biosynthetic genes, including ORF5 and ORF4, by CRISPR/dCas9 and gene refactoring, may increase the yields of WAP-8294A1, A2 and A4 four to nine times[28]. The previous ORF5 disruption mutant, which was generated by a single crossover of the plasmid construct, may undergo a second crossover, leading to a revertant (wild type) that would produce WAP-8294As[19]. On the other hand, the previous ORF6 disruption mutant led to loss of the WAP-8294A compounds, suggesting that the insertion of the whole plasmid construct into ORF6 could also have disrupted the potential promoter of the essential genes (ORFs 1–5, Fig. 1). This is likely because ORF6 lies directly upstream of ORFs 1–5 that are organized as an operon and transcriptionally coupled.

ORF4 is homologous to taurine catabolism dioxygenase, a nonheme iron 2-ketoglutarate-dependent oxygenase. We have tried to demonstrate its function through heterologous gene expression in *E. coli* and *in vitro* enzyme assays. We were able to obtain purified ORF4 protein. However, *in vitro* enzyme

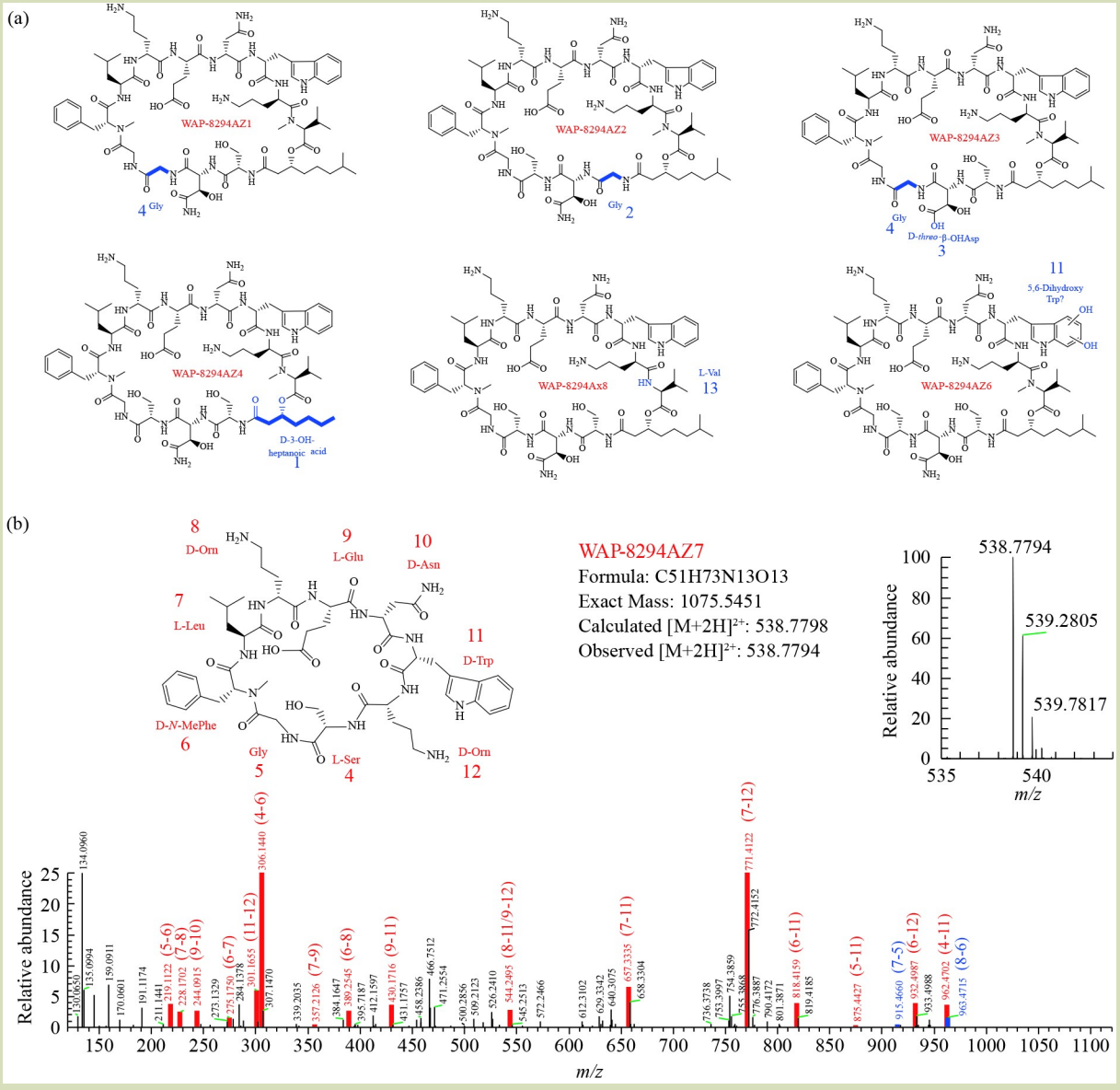

Fig. 6 Chemical structure of new WAP-8294A compounds identified in this study (a) and high-resolution MS/MS fragment analysis of an unusual WAP-8294A analog, AZ7 (b). Details of HR-MS/MS fragments of the six compounds are included in Table S2. Note that compound AZ5 is the same as Ax8[25], and the structural variations in the new compounds versus WAP-8294A2 are highlighted. In the MS/MS of AZ7, the numbers inside the parentheses indicate the position of the building blocks, the amino acid residues #4-12 of WAP-8294A2.

assays indicate that the enzyme would not use free asparagine (either D- or L-) as substrate, as seen in β-hydroxylation in calcium-dependent antibiotics[36]. This result indicates that the β-hydroxylation of the asparagine residue may take place after the amino acid has been covalently loaded to the NPRS assembly line, as seen in the β-hydroxylation of histidine in the biosynthesis of nikkomycin antibiotics[37]. We subsequently expressed the A (adenylation) domain and PCP (peptidyl carrier protein) domain of WAPS1 (see Fig. 1) that are responsible for the activation and incorporation of asparagine during NRPS-catalyzed peptide chain biosynthesis[19]. However, the heterologously expressed NRPS A-PCP proteins were insoluble, despite multiple attempts with various expression systems. As an alternative, we took the *in vivo* approach to tackle the function of ORF4 and meantime to generate new *Lysobacter* strains that could remain biosynthetically viable. We generated single-point mutants at the active sites of ORF4, which had only one amino acid change and contained no foreign DNA. LC-MS analysis indicates that WAP-8294A-like compounds were produced by

the new *Lysobacter* strains (Fig. 4). The high-resolution MS of the minor compounds confirms the deoxy analogs of parent WAP-8294A compounds. Further analysis using UHPLC-HR-MS/MS shows that the deoxy analogs lack the β-hydroxy group of the D-Asn residue, rather than on the β-hydroxy group of the fatty acid chain (Fig. 5, Figs. S3–S4, Table S2). After determining that the point mutants produced the deoxy analogs we returned to the in-frame deletion mutant and also detected the deoxy analogs using high-resolution technology (Fig. 5). The results suggest that, while ORF4 is required for the β-hydroxylation, inactivation of this gene led to extremely poor yields, indicating that a functional ORF4 is important to the overall operon to function properly. Nevertheless, our finding indicates that deoxy-WAP-8294A compounds may be produced by biosynthetic gene manipulations in *Lysobacter*, albeit in a rather low yield currently. Previously, WAP-8294A2 and its deoxy analog deoxy-WAP-8294A2 have been chemically synthesized[18]. The work shows that deoxy-WAP-8294A2 is also a potent antibacterial compound. However, the chemical approach is unlikely to be practical because it required 27 steps of highly elaborated chemical reactions. The biosynthetic approach may provide a viable alternative if the yield can be increased in the future.

Although previous studies indicate that the WAP-8294A family may contain > 19 closely related compounds, only WAP-8294A1, A2, A4, Ax8, Ax9, and Ax13 had been identified[24–26]. Here, we used UHPLC-HR-MS/MS to analyze the metabolites from *L. enzymogenes* OH11 and identified six new compounds, WAP-8294AZ1, AZ2, AZ3, AZ4, AZ6, and AZ7, in addition to four known compounds, A1, A2, A4, and Ax8 (AZ5) (Fig. 6, Table 1). The new compounds contain either a change in amino acid residues (AZ1, AZ2, AZ3, and AZ6) or a varied D-3-OH fatty acid (AZ4) (Fig. 1). Most notably, AZ7 contains only nine amino acid residues (#4-12) of A2 (Fig. 6). The composition and sequence of the nine amino acid residues of AZ7 are identical to that of the fourth through twelfth residues of WAP-8294A2. This truncated structure suggests that AZ7 may be a degradation product of the parent compounds, as seen in the recently reported lysocin-7, which is likely derived from a degradation of the parent lysocins, a family of cyclic lipodepsipeptides produced by *Lysobacter* sp. strain 3655[38]. Alternatively, AZ7 might be an aberrant biosynthetic product of the WAP biosynthetic enzymes, due to an unusual start (from #4 L-Ser) and premature release of the peptide from the NRPS assembly line, through a cyclization between #4 L-Ser and #12 D-Orn. Natural products resulting from an unusual start and release of a peptide precursor from the NRPS assembly line have been observed in other *Lysobacter* NPRS[39]. Further investigations are needed to decipher the mechanism of AZ7 formation.

5 CONCLUSIONS

With the constant emergence of resistant pathogens and the recognized risks of toxic pesticides to human health and the environment, the search for safe and effective alternative strategies for pest control has become increasingly important. Biological control measures can provide environmentally-sustainable and effective management tools for crop diseases. One key factor in the success of this biological approach is the discovery of new microbial strains that can produce potent natural products with novel chemistry and mode of action. *Lysobacter* represents a group of underexplored biocontrol agents with demonstrated efficacy and proficiency in producing bioactive natural products. The present study shows that *Lysobacter* strains can be generated to produce new antibacterial WAP-8294A compounds through minimum manipulation of the biosynthetic genes, without introducing foreign DNA. The work lays the foundation for future efforts to engineer the WAP biosynthetic pathway for yield increase of the new compounds and to develop *Lysobacter* strains as a safe and effective tool for management of crop diseases.

Supplementary materials

The online version of this article at https://doi.org/10.15302/J-FASE-2021410 contains supplementary materials (Tables S1–S2, Figs. S1–S4).

Acknowledgements

This study was supported in part by University of Nebraska Collaboration Initiative Seed Grant. Jing Zhu and Yuan Chen were recipients of a China Scholarship Council fellowship.

Compliance with ethics guidelines

Jing Zhu, Yuan Chen, and Liangcheng Du declare that they have no conflicts of interest or financial conflicts to disclose. This article does not contain any study with human or animal subjects performed by any of the authors.

REFERENCES

1. Christensen P, Cook F D. *Lysobacter*, a new genus of non-fruiting, gliding bacteria with a high base ratio. *International Journal of Systematic Bacteriology*, 1978, **28**(3): 367–393
2. Xie Y, Wright S, Shen Y, Du L. Bioactive natural products from *Lysobacter*. *Natural Product Reports*, 2012, **29**(11): 1277–1287
3. Giesler L J, Yuen G Y. Evaluation of *Stenotrophomonas maltophilia* strain C3 for biocontrol of brown patch disease. *Crop Protection*, 1998, **17**(6): 509–513
4. Sullivan R F, Holtman M A, Zylstra G J, White J F Jr, Kobayashi D Y. Taxonomic positioning of two biological control agents for plant diseases as *Lysobacter enzymogenes* based on phylogenetic analysis of 16S rDNA, fatty acid composition and phenotypic characteristics. *Journal of Applied Microbiology*, 2003, **94**(6): 1079–1086
5. Zhang Z, Yuen G Y. Biological control of *Bipolaris sorakiniana* on tall fescue by *Stenotrophomonas maltophilia* strain C3. *Phytopathology*, 1999, **89**(9): 817–822
6. Yuen G Y, Steadman J R, Lindgren D T, Schaff D, Jochum C. Bean rust biological control using bacterial agents. *Crop Protection*, 2001, **20**(5): 395–402
7. Jochum C C, Osborne L E, Yuen G Y. Fusarium head blight biological control with *Lysobacter enzymogenes*. *Biological Control*, 2006, **39**(3): 336–344
8. Kobayashi D Y, Reedy R M, Palumbo J D, Zhou J M, Yuen G Y. A *clp* gene homologue belonging to the *Crp* gene family globally regulates lytic enzyme production, antimicrobial activity, and biological control activity expressed by *Lysobacter enzymogenes* strain C3. *Applied and Environmental Microbiology*, 2005, **71**(1): 261–269
9. Li S, Du L, Yuen G, Harris S D. Distinct ceramide synthases regulate polarized growth in the filamentous fungus *Aspergillus nidulans*. *Molecular Biology of the Cell*, 2006, **17**(3): 1218–1227
10. Yu F, Zaleta-Rivera K, Zhu X, Huffman J, Millet J C, Harris S D, Yuen G, Li X C, Du L. Structure and biosynthesis of heat-stable antifungal factor (HSAF), a broad-spectrum antimycotic with a novel mode of action. *Antimicrobial Agents and Chemotherapy*, 2007, **51**(1): 64–72
11. Li S, Jochum C C, Yu F, Zaleta-Rivera K, Du L, Harris S D, Yuen G Y. An antibiotic complex from *Lysobacter enzymogenes* strain C3: antimicrobial activity and role in plant disease control. *Phytopathology*, 2008, **98**(6): 695–701
12. Lou L, Qian G, Xie Y, Hang J, Chen H, Zaleta-Rivera K, Li Y, Shen Y, Dussault P H, Liu F, Du L. Biosynthesis of HSAF, a tetramic acid-containing macrolactam from *Lysobacter enzymogenes*. *Journal of the American Chemical Society*, 2011, **133**(4): 643–645
13. Li Y, Chen H, Ding Y, Xie Y, Wang H, Cerny R L, Shen Y, Du L. Iterative assembly of two separate polyketide chains by the same single-module bacterial polyketide synthase in the biosynthesis of HSAF. *Angewandte Chemie International Edition*, 2014, **53**(29): 7524–7530
14. Li Y, Wang H, Liu Y, Jiao Y, Li S, Shen Y, Du L. Biosynthesis of the polycyclic system in the antifungal HSAF and analogues from *Lysobacter enzymogenes*. *Angewandte Chemie International Edition*, 2018, **57**(21): 6221–6225
15. Lee W, Schaefer K, Qiao Y, Srisuknimit V, Steinmetz H, Müller R, Kahne D, Walker S. The mechanism of action of lysobactin. *Journal of the American Chemical Society*, 2016, **138**(1): 100–103
16. Hashizume H, Igarashi M, Hattori S, Hori M, Hamada M, Takeuchi T. Tripropeptins, novel antimicrobial agents produced by *Lysobacter* sp. I. Taxonomy, isolation and biological activities. *Journal of Antibiotics*, 2001, **54**(12): 1054–1059
17. Hashizume H, Hirosawa S, Sawa R, Muraoka Y, Ikeda D, Naganawa H, Igarashi M. Tripropeptins, novel antimicrobial agents produced by *Lysobacter* sp. *Journal of Antibiotics*, 2004, **57**(1): 52–58
18. Itoh H, Tokumoto K, Kaji T, Paudel A, Panthee S, Hamamoto H, Sekimizu K, Inoue M. Total synthesis and biological mode of action of WAP-8294A2: a menaquinone-targeting antibiotic. *Journal of Organic Chemistry*, 2018, **83**(13): 6924–6935
19. Zhang W, Li Y, Qian G, Wang Y, Chen H, Li Y Z, Liu F, Shen Y, Du L. Identification and characterization of the anti-methicillin-resistant *Staphylococcus aureus* WAP-8294A2 biosynthetic gene cluster from *Lysobacter enzymogenes* OH11. *Antimicrobial Agents and Chemotherapy*, 2011, **55**(12): 5581–5589
20. Hamamoto H, Urai M, Ishii K, Yasukawa J, Paudel A, Murai M, Kaji T, Kuranaga T, Hamase K, Katsu T, Su J, Adachi T, Uchida R, Tomoda H, Yamada M, Souma M, Kurihara H, Inoue M, Sekimizu K. Lysocin E is a new antibiotic that targets menaquinone in the bacterial membrane. *Nature Chemical Biology*, 2015, **11**(2): 127–133
21. Murai M, Kaji T, Kuranaga T, Hamamoto H, Sekimizu K, Inoue M. Total synthesis and biological evaluation of the antibiotic lysocin E and its enantiomeric, epimeric, and N-demethylated analogues. *Angewandte Chemie International Edition*, 2015, **54**(5): 1556–1560
22. Itoh H, Tokumoto K, Kaji T, Paudel A, Panthee S, Hamamoto H, Sekimizu K, Inoue M. Development of a high-throughput strategy for discovery of potent analogues of antibiotic lysocin E. *Nature Communications*, 2019, **10**(1): 2992
23. Sang M, Wang H, Shen Y, Rodrigues de Almeida N, Conda-Sheridan M, Li S, Li Y, Du L. Identification of an anti-MRSA cyclic lipodepsipeptide, WBP-29479A1, by genome mining of *Lysobacter antibioticus*. *Organic Letters*, 2019, **21**(16): 6432–6436
24. Kato A, Nakaya S, Ohashi Y, Hirata H, Fujii K, Harada K. WAP-8294A(2), a novel anti-MRSA antibiotic produced by *Lysobacter* sp. *Journal of the American Chemical Society*, 1997, **119**(28): 6680–6681

25. Kato A, Nakaya S, Kokubo N, Aiba Y, Ohashi Y, Hirata H, Fujii K, Harada K. A new anti-MRSA antibiotic complex, WAP-8294A. I. Taxonomy, isolation and biological activities. *Journal of Antibiotic*, 1998, **51**(10): 929–935
26. Kato A, Hirata H, Ohashi Y, Fujii K, Mori K, Harada K. A new anti-MRSA antibiotic complex, WAP-8294A II. Structure characterization of minor components by ESI LCMS and MS/MS. *Journal of Antibiotics*, 2011, **64**(5): 373–379
27. Wang Y, Qian G, Liu F, Li Y Z, Shen Y, Du L. Facile method for site-specific gene integration in *Lysobacter enzymogenes* for yield improvement of the anti-MRSA antibiotics WAP-8294A and the antifungal antibiotic HSAF. *ACS Synthetic Biology*, 2013, **2**(11): 670–678
28. Yu L, Su W, Fey P D, Liu F, Du L. Yield improvement of the anti-MRSA antibiotics WAP-8294A by CRISPR/dCas9 combined with refactoring self-protection genes in *Lysobacter enzymogenes* OH11. *ACS Synthetic Biology*, 2018, **7**(1): 258–266
29. Aron A T, Gentry E C, McPhail K L, Nothias L F, Nothias-Esposito M, Bouslimani A, Petras D, Gauglitz J M, Sikora N, Vargas F, van der Hooft J J J, Ernst M, Kang K B, Aceves C M, Caraballo-Rodríguez A M, Koester I, Weldon K C, Bertrand S, Roullier C, Sun K, Tehan R M, Boya P C A, Christian M H, Gutiérrez M, Ulloa A M, Tejeda Mora J A, Mojica-Flores R, Lakey-Beitia J, Vásquez-Chaves V, Zhang Y, Calderón A I, Tayler N, Keyzers R A, Tugizimana F, Ndlovu N, Aksenov A A, Jarmusch A K, Schmid R, Truman A W, Bandeira N, Wang M, Dorrestein P C. Reproducible molecular networking of untargeted mass spectrometry data using GNPS. *Nature Protocols*, 2020, **15**(6): 1954–1991
30. Wang M, Carver J J, Phelan V V, Sanchez L M, Garg N, Peng Y, Nguyen D D, Watrous J, Kapono C A, Luzzatto-Knaan T, Porto C, Bouslimani A, Melnik A V, Meehan M J, Liu W T, Crüsemann M, Boudreau P D, Esquenazi E, Sandoval-Calderón M, Kersten R D, Pace L A, Quinn R A, Duncan K R, Hsu C C, Floros D J, Gavilan R G, Kleigrewe K, Northen T, Dutton R J, Parrot D, Carlson E E, Aigle B, Michelsen C F, Jelsbak L, Sohlenkamp C, Pevzner P, Edlund A, McLean J, Piel J, Murphy B T, Gerwick L, Liaw C C, Yang Y L, Humpf H U, Maansson M, Keyzers R A, Sims A C, Johnson A R, Sidebottom A M, Sedio B E, Klitgaard A, Larson C B, Boya P C A, Torres-Mendoza D, Gonzalez D J, Silva D B, Marques L M, Demarque D P, Pociute E, O'Neill E C, Briand E, Helfrich E J N, Granatosky E A, Glukhov E, Ryffel F, Houson H, Mohimani H, Kharbush J J, Zeng Y, Vorholt J A, Kurita K L, Charusanti P, McPhail K L, Nielsen K F, Vuong L, Elfeki M, Traxler M F, Engene N, Koyama N, Vining O B, Baric R, Silva R R, Mascuch S J, Tomasi S, Jenkins S, Macherla V, Hoffman T, Agarwal V, Williams P G, Dai J, Neupane R, Gurr J, Rodríguez A M C, Lamsa A, Zhang C, Dorrestein K, Duggan B M, Almaliti J, Allard P M, Phapale P, Nothias L F, Alexandrov T, Litaudon M, Wolfender J L, Kyle J E, Metz T O, Peryea T, Nguyen D T, VanLeer D, Shinn P, Jadhav A, Müller R, Waters K M, Shi W, Liu X, Zhang L, Knight R, Jensen P R, Palsson B Ø, Pogliano K, Linington R G, Gutiérrez M, Lopes N P, Gerwick W H, Moore B S, Dorrestein P C, Bandeira N. Sharing and community curation of mass spectrometry data with Global Natural Products Social Molecular Networking. *Nature Biotechnology*, 2016, **34**(8): 828–837
31. Chambers M C, Maclean B, Burke R, Amodei D, Ruderman D L, Neumann S, Gatto L, Fischer B, Pratt B, Egertson J, Hoff K, Kessner D, Tasman N, Shulman N, Frewen B, Baker T A, Brusniak M Y, Paulse C, Creasy D, Flashner L, Kani K, Moulding C, Seymour S L, Nuwaysir L M, Lefebvre B, Kuhlmann F, Roark J, Rainer P, Detlev S, Hemenway T, Huhmer A, Langridge J, Connolly B, Chadick T, Holly K, Eckels J, Deutsch E W, Moritz R L, Katz J E, Agus D B, MacCoss M, Tabb D L, Mallick P. A cross-platform toolkit for mass spectrometry and proteomics. *Nature Biotechnology*, 2012, **30**(10): 918–920
32. Pluskal T, Castillo S, Villar-Briones A, Oresic M. MZmine 2: modular framework for processing, visualizing, and analyzing mass spectrometry-based molecular profile data. *BMC Bioinformatics*, 2010, **11**(1): 395
33. Shannon P, Markiel A, Ozier O, Baliga N S, Wang J T, Ramage D, Amin N, Schwikowski B, Ideker T. Cytoscape: a software environment for integrated models of biomolecular interaction networks. *Genome Research*, 2003, **13**(11): 2498–2504
34. Elkins J M, Ryle M J, Clifton I J, Dunning Hotopp J C, Lloyd J S, Burzlaff N I, Baldwin J E, Hausinger R P, Roach P L. X-ray crystal structure of *Escherichia coli* taurine/alpha-ketoglutarate dioxygenase complexed to ferrous iron and substrates. *Biochemistry*, 2002, **41**(16): 5185–5192
35. Chen H, Olson A S, Su W, Dussault P H, Du L. Fatty acyl incorporation in the biosynthesis of WAP-8294A, a group of potent anti-MRSA cyclic lipodepsipeptides. *RSC Advances*, 2015, **5**(128): 105753–105759
36. Strieker M, Kopp F, Mahlert C, Essen L O, Marahiel M A. Mechanistic and structural basis of stereospecific Cbeta-hydroxylation in calcium-dependent antibiotic, a daptomycin-type lipopeptide. *ACS Chemical Biology*, 2007, **2**(3): 187–196
37. Chen H, Hubbard B K, O'Connor S E, Walsh C T. Formation of beta-hydroxy histidine in the biosynthesis of nikkomycin antibiotics. *Chemistry & Biology*, 2002, **9**(1): 103–112
38. Yu L, Du F, Chen X, Zheng Y, Morton M, Liu F, Du L. Identification of the biosynthetic gene cluster for the anti-MRSA lysocins through gene cluster activation using strong promoters of housekeeping genes and production of new analogs in *Lysobacter* sp. 3655. *ACS Synthetic Biology*, 2020, **9**(8): 1989–1997
39. Li S, Wu X, Zhang L, Shen Y, Du L. Activation of a cryptic gene cluster in *Lysobacter enzymogenes* reveals a module/domain portable mechanism of nonribosomal peptide synthetases in the biosynthesis of pyrrolopyrazines. *Organic Letters*, 2017, **19**(19): 5010–5013